

Research on Atmospheric Motion in Horizontal Discrete Grids

LIU Yudi^{*1,2} (刘宇迪), WANG Bin¹ (王斌), and JI Zhongzhen¹ (季仲贞)

¹*LASG, Institute of Atmospheric Physics, Chinese Academy of Sciences, Beijing 100029*

²*Institute of Meteorology, PLA University of Sciences and Engineering, Nanjing 211101*

(Received January 13, 2002; revised November 4, 2002)

ABSTRACT

Starting from the linear shallow-water equations and using Arakawa A-E and Z grids, a study is made of inertia-gravitational and Rossby waves in the six grids from the perspectives of frequency and group velocity. Results indicate that grids C, Z, and F thereof give smaller distortion compared to the others.

Key words: grid dispersion property, Rossby wave, inertia-gravitational wave, group velocity

1. Introduction

As we know, atmospheric motion may be divided into two stages, adaptive and developing, being described by the inertia-gravitational and Rossby waves, respectively (McHale, 1993a, b). In employing a numerical model to simulate atmospheric motion, the problem arises of discretizing the variables of the atmospheric states, i.e., configuring or arranging the variables. Horizontal discrete grids in current use are the Arakawa A-E and Z (David, 1994) grids. It is a problem awaiting further study to determine which of the grids is/are able to depict successfully both inertia-gravitational and Rossby waves. Suppose we find a grid which applies well to the former case but fails to describe the latter. That means that its description of the atmospheric evolution is a failure because the future trend of the event is not fully revealed. In the same way, a grid that can depict well a Rossby wave but is unable to simulate the adjustment or adaptive process, i.e., change in weather process, does not serve our purpose either.

Winninghoff (1968) and Arakawa and Lamb (1977) studied inertia-gravitational waves solely in the grids of Arakawa A-E, and thought that for resolvable models grid C is the best. Following their ideas, Liu et al. (2001a) further investigated them in Arakawa A-E and Z. And Liu et al. (2001b; 2002) investigated only Rossby waves in these grids. Exploration of both waves in combination has not been attempted, however. For this reason, an effort is made in this article to imitate both waves in these grids, starting from the linear shallow-water equations, followed by a comparison between numerical and analytical solutions from the perspectives of frequency and group velocity (Collatz,

1996; Fox-Rabinovitz, 1991; Song and Tang, 1993; Wajsowicz, 1986) in order to determine which of these grids is most suitable for our purpose.

To investigate all aspects of both waves in the six Arakawa grids, this article presents analytical dispersion and horizontal group velocity component formulations for describing inertia-gravitational and Rossby waves, starting from the shallow-water equations (section 2) and their related numerical expressions (section 3). A comprehensive discussion of the numerical expressions is given in section 4 with a conclusion in section 5.

2. Differential form

2.1 Rossby wave

Equations for depicting Rossby waves under quasi-geostrophic β -plane approximation are

$$fv_g - g \frac{\partial h}{\partial x} = 0, \quad (1)$$

$$fu_g + g \frac{\partial h}{\partial y} = 0, \quad (2)$$

$$\frac{\partial u_g}{\partial t} - fv_a - \beta v_g y = 0, \quad (3)$$

$$\frac{\partial v_g}{\partial t} + fu_a + \beta u_g y = 0, \quad (4)$$

$$\frac{\partial h}{\partial t} + H \left(\frac{\partial u_a}{\partial x} + \frac{\partial v_a}{\partial y} \right) = 0, \quad (5)$$

where u_g and v_g (u_a and v_a) signify geostrophic (ageostrophic) velocity components in the zonal and meridional extent, respectively, h the displacement, y the meridional distance, $\beta = \partial f / \partial y$, and f and β are set as constants.

*E-mail: yd.liu0509@yahoo.com.cn

Assume the Rossby wave is on a plane with the wave solution, $F = \bar{F}e^{i(kx+ly-wt)}$, where F' denotes a physical quantity whose amplitude is given by \bar{F} . Inserting the wave solution into Eq.(1-5) yields a precise dispersion relation

$$\omega = -\frac{\beta\lambda^2 k}{1 + \lambda^2(k^2 + l^2)}. \quad (6)$$

For the comparison to numerical dispersion relations from the six grids to follow, (6) is rewritten as

$$\left(\frac{\omega}{\beta d}\right)_{\text{diff}} = -\frac{(\lambda/d)^2 kd}{1 + (\lambda/d)^2[(kd)^2 + (ld)^2]}, \quad (7)$$

where $k(l)$ is the zonal (meridional) wavenumber, $\lambda = \sqrt{gH}/f$ the Rossby deformation radius, and d the grid length.

We see from (7) that the analytical frequency is negative for the wave at any interval.

It is necessary to address, separately, the Group Velocity Component (GVC) both in the x and y direction since the Rossby wave is anisotropic. Then we get the GVC in both directions through (7), i.e.,

$$C_{gx,\text{diff}} = \frac{2k^2\beta\lambda^4}{\{(1 + (\lambda/d)^2[(kd)^2 + (ld)^2])^2\}} - \frac{\beta\lambda^2}{1 + (\lambda/d)^2[(kd)^2 + (ld)^2]},$$

$$C_{gy,\text{diff}} = \frac{2kl\beta\lambda^4}{\{(1 + (\lambda/d)^2[(kd)^2 + (ld)^2])^2\}},$$

in which the subscript $gx(gy)$ of C on the left-hand side denotes the GVC in the $x(y)$ direction and the superscript diff the differential representation.

The y -axis GVC expression shows that the Group Velocity (GV) of the wave at any interval diminishes versus augmented wavenumber. Owing to the fact that the x -axis GVC formulation is rather complicated, the wavenumber-dependent variations are hard to see clearly in a direct manner. A detailed discussion is deferred to the next section.

2.2 Inertia-gravitational wave

The differential shallow-water equations for an f -plane inertia-gravitational wave have the form

$$\frac{\partial u}{\partial t} - fv + g\frac{\partial h}{\partial x} = 0, \quad (8)$$

$$\frac{\partial v}{\partial t} + fu + g\frac{\partial h}{\partial y} = 0, \quad (9)$$

$$\frac{\partial h}{\partial t} + H\left(\frac{\partial u}{\partial x} + \frac{\partial v}{\partial y}\right) = 0, \quad (10)$$

where u and v are velocity components in the x and y direction, respectively, and h the displacement from steady depth H .

Set h approximately to be $e^{i(kx+ly-wt)}$ and we find

the analytical dispersion relation

$$\left(\frac{\omega}{f}\right)^2 = 1 + \left(\frac{\lambda}{d}\right)^2[(kd)^2 + (ld)^2], \quad (11)$$

in which k and l stand for the horizontal wavenumber in zonal and meridional extent, respectively, $\lambda = \sqrt{gH}/f$ for the Rossby deformation radius, and d for grid spacing. The frequency increases as a function of wavenumber.

GVC are also derived from (11), and because the inertia-gravitational wave is isotropic, we take the GVC only in the x direction for all the grids under study. The x -axis GVC has the form

$$C_{gx,\text{diff}} = \frac{fk\lambda^2}{\sqrt{1 + (\lambda/d)^2[(kd)^2 + (ld)^2]}}, \quad (12)$$

from which we notice that the GVC is always positive over the full range of the horizontal scales.

3. Dispersion properties calculated in horizontal discrete grids

3.1 Rossby wave

Equations (1)-(5) is discretized separately on the 6 grids, with the distribution of the respective variables shown in Fig. 1. The thinking is much the same in solving the dispersion equations for Arakawa A-E grids in such a way as to assume a wave solution $F = \bar{F}e^{i(ki\Delta x + lj\Delta y - wt)}$, with i and j denoting the i th and j th gridpoint in the x and y extent, respectively. The wave solution, when substituted into the difference equations, leads to a dispersion expression for each of the grids, as indicated in Table 1. For Arakawa Z, on the other hand, we have to proceed from Eqs. (1)-(5) to derive, with the aid of vorticity and divergence, the following formulations

$$f\zeta_g = g\left(\frac{\partial^2 h}{\partial x^2} + \frac{\partial^2 h}{\partial y^2}\right),$$

$$\frac{\partial \zeta_g}{\partial t} + f\delta + \frac{\beta g}{f}\frac{\partial h}{\partial x} = 0,$$

$$\frac{\partial h}{\partial t} + H\delta = 0,$$

and then write the discrete equations based upon the configuration of variables

$$f\zeta_g - g(h_{xx} + h_{yy}) = 0,$$

$$\frac{\partial \zeta_g}{\partial t} + f\delta + \frac{\beta g}{f}h_x^x = 0,$$

$$\frac{\partial h_g}{\partial t} + H\delta = 0,$$

This results in a dispersion expression of grid Z by means of a set wave solution (refer again to Table 1).

We notice therefrom that the frequencies obtained from these grids are not always negative for the wave at any interval, as in the analytical case, i.e., positive frequency is possible in some intervals. In view of the

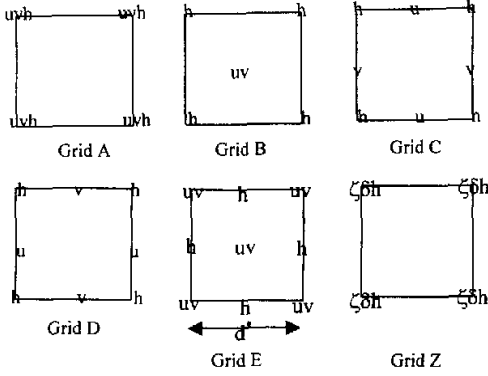


Fig. 1. Definitions of the 6 square Arakawa grids with $u(v)$ giving the horizontal velocity component in the zonal (meridional) direction, h the geopotential height, d the grid spacing, $d^* = \sqrt{2}d$, and ζ_g and δ the geostrophic vorticity and divergence, respectively.

fact that these dispersion equations are too complicated for us to compare them in a visual fashion, we shall present 3D representations in section 4 for this purpose.

On the other hand, the GV components are not negligible quantities, denoting numerical properties of the grids so that the horizontal components are computed as shown in Tables 2 and 3. Therefrom, however, we cannot differentiate visually between the analytical solution and the grid (numerical) formulations, and so we show graphically the differences in section 4.

3.2 Inertia-gravitational wave

The same procedure is undertaken for the inertia-gravitational wave as in the case of the Rossby wave (see previous subsection) yielding the corresponding dispersion equations shown in Table 4.

Because of the isotropicity of this study wave we take into account only the GVC in the x direction (see Table 5).

4. Discussion

Here we shall compare graphically the frequencies

Table 1. Dispersion equations versus the analytical solution (AS) for Rossby waves on Arakawa grids

AS/Grid	Dispersion equation
AS	$\left(\frac{\omega}{\beta d}\right)_{\text{diff}} = -\frac{(\lambda/d)^2 kd}{1 + (\lambda/d)^2 [(kd)^2 + (ld)^2]}$
Grid A	$\left(\frac{\omega}{\beta d}\right)_A = -\frac{(\lambda/d)^2 \sin kd \cos ld}{1 + (\lambda/d)^2 [\sin^2 kd + \sin^2 ld]}$
Grid B	$\left(\frac{\omega}{\beta d}\right)_B = -\frac{(\lambda/d)^2 \sin kd}{1 + 2(\lambda/d)^2 [1 - \cos kd \cos ld]}$
Grid C	$\left(\frac{\omega}{\beta d}\right)_C = -\frac{(\lambda/d)^2 \sin kd \cos^2(ld/2)}{\cos^2(kd/2) \cos^2(ld/2) + 4(\lambda/d)^2 [\sin^2(kd/2) + \sin^2(ld/2)]}$
Grid D	$\left(\frac{\omega}{\beta d}\right)_D = -\frac{(\lambda/d)^2 \sin kd \cos^2(ld/2)}{1 + 4(\lambda/d)^2 [\sin^2(kd/2) + \sin^2(ld/2)]}$
Grid E	$\left(\frac{\omega}{\beta d}\right)_E = -\frac{\sqrt{2}(\lambda/2)^2 \sin(kd/\sqrt{2}) \cos(ld/\sqrt{2})}{1 + 2(\lambda/d)^2 [\sin^2(kd/\sqrt{2}) + \sin^2(ld/\sqrt{2})]}$
Grid Z	$\left(\frac{\omega}{\beta d}\right)_Z = -\frac{(\lambda/2)^2 \sin kd}{1 + 4(\lambda/d)^2 [\sin^2(kd/2) + \sin^2(ld/2)]}$

Table 2. The x -axis GVC on Arakawa grids vs analytical solution (AS) for Rossby waves

AS/Grid	x -axis Group Velocity Component
AS	$C_{gx,\text{diff}} = \frac{2k^2 \beta \lambda^4}{\{1 + (\lambda/d)^2 [(kd)^2 + (ld)^2]\}^2} - \frac{\beta \lambda^2}{1 + (\lambda/d)^2 [(kd)^2 + (ld)^2]}$
Grid A	$C_{gx,A} = \frac{2\beta \lambda^4 \cos kd \cos ld \sin^2 kd}{d^2 \{1 + (\lambda/d)^2 [\sin^2 kd + \sin^2 ld]\}^2} - \frac{\beta \lambda^2 \cos kd \cos ld}{1 + (\lambda/d)^2 [\sin^2 kd + \sin^2 ld]}$
Grid B	$C_{gx,B} = \frac{\beta \lambda^2 \cos kd}{1 + 2(\lambda/d)^2 [1 - \cos kd \cos ld]} - \frac{2\beta \lambda^4 \cos ld \sin^2 kd}{d^2 \{1 + 2(\lambda/d)^2 [1 - \cos kd \cos ld]\}^2}$

Table 2. (Continued)

AS/Grid	<i>x</i> -axis Group Velocity Component
Grid C	$C_{gx,C} = \frac{\beta\lambda^2 \sin kd \cos^2 \frac{ld}{2} \left(\frac{2\lambda^2 \sin kd}{d} - \frac{d}{2} \sin kd \cos^2 \frac{ld}{2} \right)}{d \{ \cos^2(kd/2) \cos^2(ld/2) + 4(\lambda/d)^2 [\sin^2(kd/2) + \sin^2(ld/2)] \}^2}$ $\frac{\beta\lambda^2 \cos kd \cos^2(ld/2)}{\cos^2(kd/2) \cos^2(ld/2) + 4(\lambda/d)^2 [\sin^2(kd/2) + \sin^2(ld/2)]}$
Grid D	$C_{gx,D} = \frac{2\beta\lambda^4 (\sin kd)^2 \cos^2(ld/2)}{d^2 \{ 1 + 4(\lambda/d)^2 [\sin^2(kd/2) + \sin^2(ld/2)] \}^2}$ $\frac{\beta\lambda^2 \cos kd \cos^2(ld/2)}{1 + 4(\lambda/d)^2 [\sin^2(kd/2) + \sin^2(ld/2)]}$
Grid E	$C_{gx,E} = \frac{4\beta\lambda^4 \cos(kd/\sqrt{2}) \cos(ld/\sqrt{2}) \sin^2(kd/\sqrt{2})}{d^2 \{ 1 + 2(\lambda/d)^2 [\sin^2(kd/\sqrt{2}) + \sin^2(ld/\sqrt{2})] \}^2}$ $\frac{\beta\lambda^2 \cos(kd/\sqrt{2}) \cos(ld/\sqrt{2})}{1 + 2(\lambda/d)^2 [\sin^2(kd/\sqrt{2}) + \sin^2(ld/\sqrt{2})]}$
Grid Z	$C_{gx,Z} = \frac{2\beta\lambda^4 (\sin kd)^2}{d^2 \{ 1 + 4(\lambda/d)^2 [\sin^2(kd/2) + \sin^2(ld/2)] \}^2}$ $\frac{\beta\lambda^2 \cos kd}{1 + 4(\lambda/d)^2 [\sin^2(kd/2) + \sin^2(ld/2)]}$

Table 3. As Table 2 for the *y*-axis

AS/Grid	<i>y</i> -axis Group Velocity Component
AS	$C_{gy,diff} = \frac{2kl\beta\lambda^4}{\{ 1 + (\lambda/d)^2 [(kd)^2 + (ld)^2] \}^2}$
Grid A	$C_{gy,A} = \frac{2\beta\lambda^4 \sin kd \sin ld \cos^2 ld}{d^2 \{ 1 + (\lambda/d)^2 [\sin^2 kd + \sin^2 ld] \}^2} + \frac{\beta\lambda^2 \sin kd \sin ld}{1 + (\lambda/d)^2 [\sin^2 kd + \sin^2 ld]}$
Grid B	$C_{gy,B} = \frac{\beta\lambda^4 \sin 2kd \sin ld}{d^2 \{ 1 + 2(\lambda/d)^2 [1 - \cos kd \cos ld] \}^2}$
Grid C	$C_{gy,C} = \frac{\beta\lambda^2 \sin kd \cos^2 \frac{ld}{2} \left(\frac{2\lambda^2 \sin ld}{d} - \frac{d}{2} \sin ld \cos^2 \frac{kd}{2} \right)}{d \{ \cos^2(kd/2) \cos^2(ld/2) + 4(\lambda/d)^2 [\sin^2(kd/2) + \sin^2(ld/2)] \}^2}$ $+ \frac{\frac{1}{2} \beta\lambda^2 \sin ld \sin kd}{\cos^2(kd/2) \cos^2(ld/2) + 4(\lambda/d)^2 [\sin^2(kd/2) + \sin^2(ld/2)]}$
Grid D	$C_{gy,D} = \frac{4\beta\lambda^4 \sin kd \sin \frac{ld}{2} \cos^3(ld/2)}{d^2 \{ 1 + 4(\lambda/d)^2 [\sin^2(kd/2) + \sin^2(ld/2)] \}^2}$ $+ \frac{\frac{1}{2} \beta\lambda^2 \sin kd \sin ld}{1 + 4(\lambda/d)^2 [\sin^2(kd/2) + \sin^2(ld/2)]}$
Grid E	$C_{gy,E} = \frac{4\beta\lambda^4 \sin(kd/\sqrt{2}) \sin(ld/\sqrt{2}) \cos^2(ld/\sqrt{2})}{d^2 \{ 1 + 2(\lambda/d)^2 [\sin^2(kd/\sqrt{2}) + \sin^2(ld/\sqrt{2})] \}^2}$ $+ \frac{\beta\lambda^2 \sin(kd/\sqrt{2}) \sin(ld/\sqrt{2})}{1 + 2(\lambda/d)^2 [\sin^2(kd/\sqrt{2}) + \sin^2(ld/\sqrt{2})]}$
Grid Z	$C_{gy,Z} = \frac{2\beta\lambda^4 \sin ld \sin kd}{d^2 \{ 1 + 4(\lambda/d)^2 [\sin^2(kd/2) + \sin^2(ld/2)] \}^2}$

Table 4. Dispersion formulations (numerical vs analytical solution) for inertia-gravitational waves on six grids

AS/Grid	Dispersion equation
AS	$\left(\frac{\omega}{f}\right)^2 = 1 + \left(\frac{\lambda}{d}\right)^2 [(kd)^2 + (ld)^2]$
Grid A	$\left(\frac{\omega}{f}\right)_A^2 = 1 + \left(\frac{\lambda}{d}\right)^2 [\sin^2 kd + \sin^2 ld]$
Grid B	$\left(\frac{\omega}{f}\right)_B^2 = 1 + 2\left(\frac{\lambda}{d}\right)^2 [1 - \cos kd \cos ld]$
Grid C	$\left(\frac{\omega}{f}\right)_C^2 = \cos^2 \frac{kd}{2} \cos^2 \frac{ld}{2} + 4\left(\frac{\lambda}{d}\right)^2 \left[\sin^2 \frac{kd}{2} + \sin^2 \frac{ld}{2} \right]$
Grid D	$\left(\frac{\omega}{f}\right)_D^2 = \cos^2 \frac{kd}{2} \cos^2 \frac{ld}{2} + \left(\frac{\lambda}{d}\right)^2 \left[\cos^2 \frac{kd}{2} \sin^2 ld + \cos^2 \frac{ld}{2} \sin^2 kd \right]$
Grid E	$\left(\frac{\omega}{f}\right)_E^2 = 1 + 2\left(\frac{\lambda}{d}\right)^2 \left[\sin^2 \frac{kd}{\sqrt{2}} + \sin^2 \frac{ld}{\sqrt{2}} \right]$
Grid Z	$\left(\frac{\omega}{f}\right)_Z^2 = 1 + 4\left(\frac{\lambda}{d}\right)^2 \left[\sin^2 \frac{kd}{2} + \sin^2 \frac{ld}{2} \right]$

Table 5. The x -axis GVC (grid vs AS) in the six grids for inertia-gravitational waves

AS/Grid	x -axis Group Velocity Component
AS	$C_{gx,diff} = \frac{fk\lambda^2}{\sqrt{1 + \left(\frac{\lambda}{d}\right)^2 [(kd)^2 + (ld)^2]}}$
Grid A	$C_{gx,A} = \frac{f\lambda^2 \sin 2kd}{2d\sqrt{1 + \left(\frac{\lambda}{d}\right)^2 (\sin^2 kd + \sin^2 ld)}}$
Grid B	$C_{gx,B} = \frac{f\lambda^2 \cos ld \sin kd}{d\sqrt{1 + 2\left(\frac{\lambda}{d}\right)^2 (1 - \cos kd \cos ld)}}$
Grid C	$C_{gx,C} = \frac{f\left(\frac{2\lambda^2}{d} - \frac{d}{2} \cos^2 \frac{ld}{2}\right) \sin kd}{2\sqrt{\cos^2 \frac{kd}{2} \cos^2 \frac{ld}{2} + 4\left(\frac{\lambda}{d}\right)^2 \left(\sin^2 \frac{kd}{2} + \sin^2 \frac{ld}{2}\right)}}$
Grid D	$C_{gx,D} = \frac{f\left[-\frac{d}{2} \sin kd \cos^2 \frac{ld}{2} + \frac{\lambda^2}{d} (\sin 2kd \cos^2 \frac{ld}{2} - \frac{1}{2} \sin kd \sin^2 ld)\right]}{2\sqrt{\cos^2 \frac{kd}{2} \cos^2 \frac{ld}{2} + \left(\frac{\lambda}{d}\right)^2 \left(\cos^2 \frac{kd}{2} \sin^2 ld + \cos^2 \frac{ld}{2} \sin^2 kd\right)}}$
Grid E	$C_{gx,E} = \frac{f\lambda^2 \sin 2\sqrt{2}kd/\sqrt{2}}{d\sqrt{1 + 2\left(\frac{\lambda}{d}\right)^2 \left(\sin^2 \frac{kd}{\sqrt{2}} + \sin^2 \frac{ld}{\sqrt{2}}\right)}}$
Grid Z	$C_{gx,Z} = \frac{f\lambda^2 \sin kd}{d\sqrt{1 + 4\left(\frac{\lambda}{d}\right)^2 \left(\sin^2 \frac{kd}{2} + \sin^2 \frac{ld}{2}\right)}}$

and horizontal GVCs obtained from analytical and numerical treatment based upon the equations shown in section 2 to investigate which of the grid results is closest to the AS. Thus we seek to single out one or more Arakawa grids that produces minimum error in simulating Rossby and inertia-gravitational waves.

Figure 2 portrays the dispersion relations (numerical vs AS) for the Rossby (2a) and inertia-gravitational waves (2b).

Figure 2a indicates that grid C gives the most accurate simulation of the Rossby wave, but it is only somewhat superior to the equivalents D, Z, and E, a conclusion that is in quite good agreement with Yu (1994). On the other hand, Fig.2b displays the higher ability of grids C, Z, and E to describe the inertia-gravitational wave (grid E is a bit inferior to the other two in this case). As viewed for frequency variation, grids C, Z, and E can satisfactorily depict the two

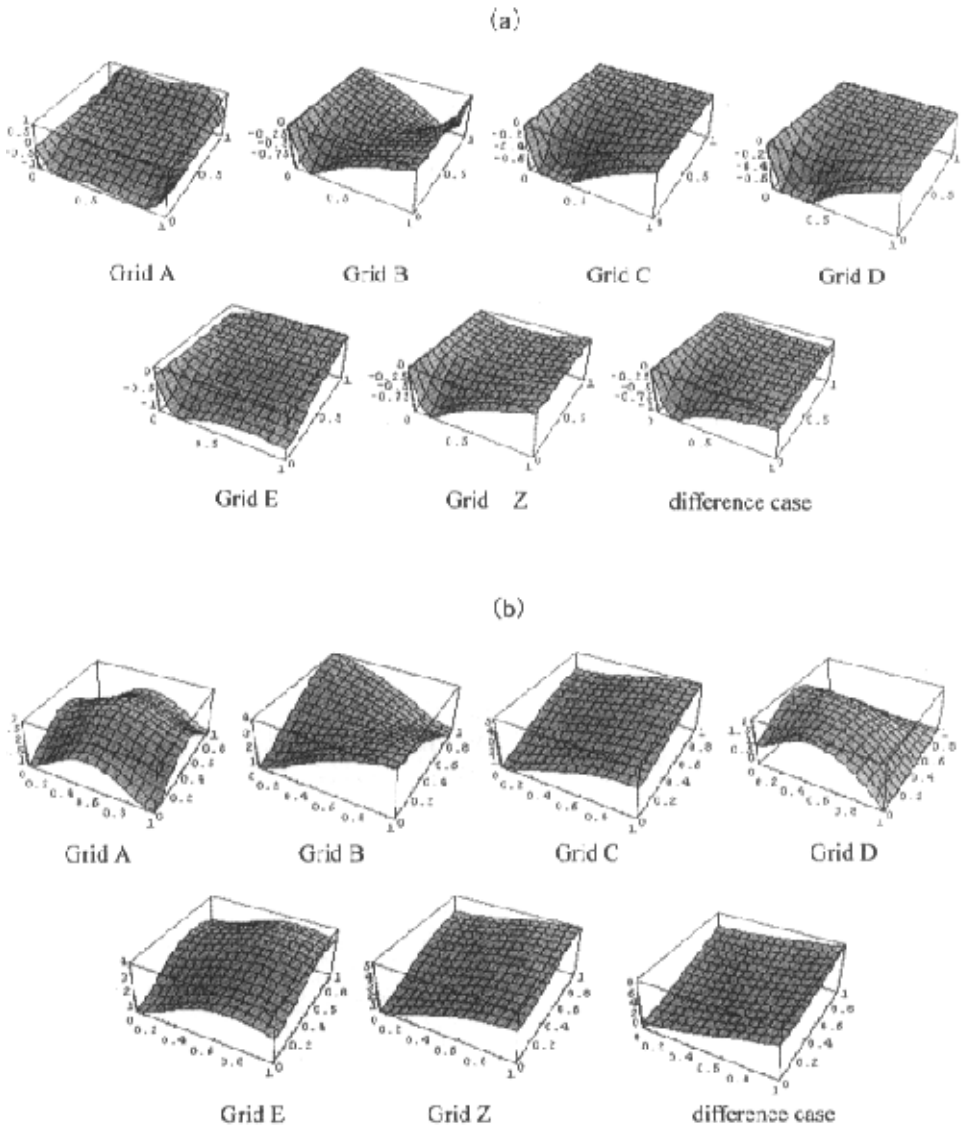


Fig. 2. (a) Visual dispersions (numerical vs AS) for the Rossby wave related to the six grids. Coordinates are kd/π in the x -, ld/π in the y -, and $\omega/\beta d$ in the z -direction; b) same as (a) except for the inertia-gravitational wave, and with ω/f as the z -axis coordinate.

types of atmospheric waves compared to grids A, B, and D.

Figure 3 shows plots of x -axis GVCs (numerical vs AS) in the Arakawa grids for the Rossby (a) and inertia-gravitational waves (b).

One sees from Fig. 3a that the simulations from

grids C, D, and Z agree in the main with the AS case and grid E expression indicates some deviation from AS only at short wave bands, suggesting that the four grids are applicable to the description of Rossby waves.

Now let us have a look at Fig.3b where greater differences occur between numerical and analytical so-

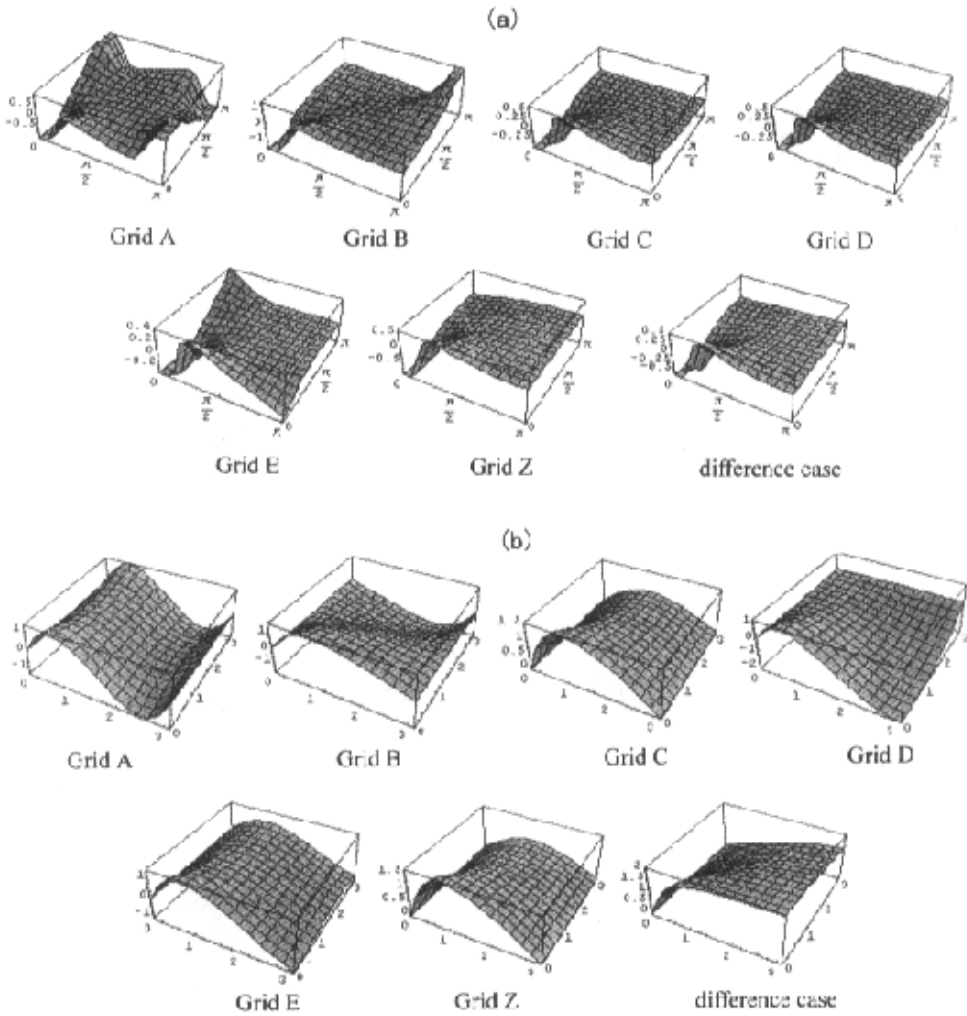


Fig. 3. (a) The x -axis GVC (numerical vs AS) for the Rossby wave in the six grids. Coordinates are kd in the x -, ld in the y -, and $C_{gx}/\beta d$ in the z -axis; (b) similar to (a) but for the inertia-gravitational wave and the z -axis denoted by C_{gx}/f .

lutions except for smaller deviations at long wave intervals for grids C, Z, and E, which exhibit a greater ability to imitate atmospheric motions as far as the x -axis GVC is considered.

Figure 4 illustrates the y -axis GVC (numerical vs AS) in the six grids for the Rossby (4a) and inertia-gravitational waves (4b).

From Fig. 4a, we notice that in the simulation of

geostrophic evolution, grids Z, D, C, and E are comparable, they agree in the main with the AS case. In Fig.4b, on the other hand, only at long wave intervals are the numerical solutions from C, Z, and E in good agreement with the AS. As viewed from the y -axis GVC, grids C, Z, and E are more suitable for the description of both kinds of atmospheric waves as compared to the equivalents A, B, and D.

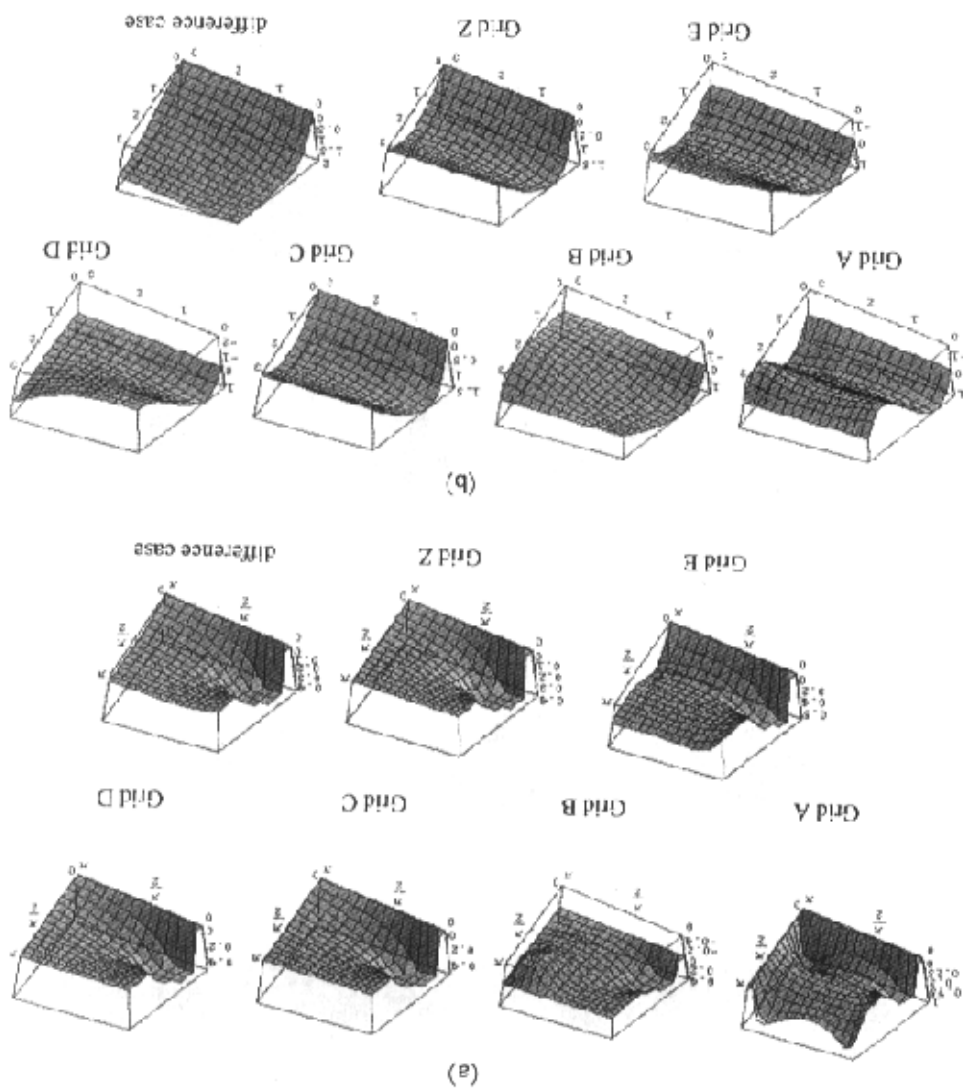


Fig. 4. The y -axis GVC (numerical vs AS) for the Rossby wave in the six grids. Coordinates are kd in the x -, ld in the y -, and $C_{gy}/\beta d$ in the z -axis; (b) same as (a) but for the inertia-gravitational wave, and with the z -axis denoted by C_{gy}/f .

Taking the frequency and horizontal GVCs together, grids C, Z, and E are better means (schemes) in the study of both atmospheric waves.

Let us now look into causes of the differences between AS and these grid expressions.

(a) Grid A is a non-staggering scheme and is easy

to deal with. Because u and v are defined at the same gridpoint, the calculated Coriolis term of the momentum equation has higher precision. However, the space derivative terms have to be averaged and so must the terms of mass convergence and divergence defined at point h . As we know, averaging definitely "hides"

noise at adopted minimum scales. For this reason, grid A is almost unusable at present.

(b) Grid B needs no averaging over the Coriolis term, but the term of pressure gradient force has to be averaged as in grid A, thereby leading to small-scale noise contained in it.

(c) Grid C necessitates no averaging of pressure force because the defined gridpoint h is between $u(v)$ points in the E-W (N-S) direction. Similarly, convergence/divergence terms of the equation of continuity require no averaging of a wind field for calculation. Nevertheless, the Coriolis term has to be averaged due to the fact that u and v are defined at different points. It is noted that for small-scale inertia-gravitational waves this term is ignorable, suggesting that grid C is quite applicable if a model has sufficiently high horizontal resolution to represent on this grid the insensitivity of a minimum scale wave to the Coriolis force. More specifically, the grid serves the purpose only when the grid spacing is smaller than the deformation radius λ .

(d) Grid D allows one to perform simple calculation of geostrophic winds but produces no accurate dispersion relation because averaging applies to the pressure force, mass convergence/divergence, and even the Coriolis term.

(e) Grid E ignore whose grid length is $d^* = \sqrt{2}d$, requires no averaging of the Coriolis force, pressure force, or mass convergence/divergence. A problem arises owing to the fact that grid E is "degraded" in one direction into grid A, and grid spacing $d = d^*/\sqrt{2}$ is reduced.

(f) Grid Z is a grid in which the component of wind divergence (rotated part) is close to a staggering scheme as in Grid C (D). This suggests that grid Z does not correspond to any of the above five grids and, besides, it necessitates no averaging of the terms involved. The Z-related equation has ∇^2 as the exclusive operator of the space difference, which emerges in its divergence equation and acts upon gridpoint h . According to the usual centered limited difference scheme, $\nabla^2 h$ has its limited differencing approximation defined at gridpoint h such that its averaging is unnecessary, thus resulting in smaller error.

5. Concluding remarks

From the above analysis we conclude that grids C, Z, and E are more suitable for the two kinds of waves,

of which C is optimal, from the perspectives of frequency and group velocity. As a result, C- and E-form grids should be adopted in the horizontal directions when developing a limited difference numerical model. The discretized treatment will produce minimum errors.

Acknowledgments. This work was sponsored by the program "Major Directions of Renewed Research Lines, Chinese Academy of Sciences (KZCX2208)".

REFERENCES

- Arakawa, A., and V. R. Lamb, 1977: Computational dynamic processes of UCLA general circulation model. *Methods in Computational Physics*, J. Chang, Ed., Academic Press, 173-256.
- Collatz, L., 1966: *The Numerical Treatment of Differential Equations*. Springer-Verlag, New York, 381 pp.
- David, A. R., 1994: Geostrophic adjustment and the finite difference shallow water equations. *Mon. Wea. Rev.*, **122**, 1371-1377.
- Fox-Rabinovitz, M., 1991: Computational dispersion of horizontal staggered grids for atmospheric and ocean models. *Mon. Wea. Rev.*, **119**, 1624-1639.
- Liu Y. D., Gui Q. J., Li X. D., and Zhu H. W., 2001a: Study on dispersion features as calculated in horizontal grids. *Quart. J. Appl. Meteor.*, **12**(2), 140-149.
- Liu Y. D., Ji Z. Z., Zhu H. W., Li X. D., and Hou Z. M., 2001b: Effects of horizontal grids on Rossby wave. *Acta Meteorologica Sinica*, **60**(1), 76-84.
- Liu Y. D., Ji Z. Z., and Wang B., 2002: Computational dispersion properties of vertical staged grids in non-hydrostatic models. *Advances in Atmospheric Sciences*, **19**(3), 524-548.
- McHall, Y. L., 1993a: Large scale perturbations in extratropical atmosphere, Part I: On Rossby waves. *Advances in Atmospheric Sciences*, **10**(2), 169-180.
- McHall, Y. L., 1993b: Large scale perturbations in extratropical atmosphere, Part II: On geostrophic waves. *Advances in Atmospheric Sciences*, **10**(2), 181-192.
- Wajswicz, R.C., 1986: Free planetary waves in finite-difference numerical models. *J. Phys. Oceanogr.*, **16**, 773-789.
- Winninghoff, F. J., 1968: On the adjustment towards a geostrophic balance in a simple primitive equation model with application to the problems and objective analysis. Ph. D. dissertation University of California, Los Angeles, 161 pp.
- Yang, S., and T. Tang, 1993: Dispersion and group velocity in numerical schemes for three-dimensional hydrodynamic equation. *J. Comput. Phys.*, **105**, 72-82.
- Yu R. C., 1994: Properties of difference schemes under the distribution of grid E variables. *Scientia Atmospherica Sinica*, **18**(2), 152-162. (in Chinese)

水平离散网格与大气运动

刘宇迪 王 斌 季仲贞

摘 要

从线性浅水方程组出发, 在Arakawa A-E网格和Z网格上, 从频率和群速方面讨论了这六种网格对大气中的两种重要的波动: 惯性重力波和Rossby波的描述能力。结果表明: C、Z、E网格比其它网格产生的歪曲都要小。

关键词: 网格, 频散特征, Rossby波, 惯性重力波, 群速